Impact of Source Model on Earthquake Hazard and Insurance Risk in New Zealand

D. Fitzenz, E. Apel, M. Drayton, & M. Nyst

RMS Inc., Newark, California, USA.

2015 NZSEE
Conference

ABSTRACT: RMS is updating its earthquake insurance risk model for New Zealand. We examine the impact on risk from changing the hazard component of the model. The previous RMS hazard model is based on the 2002 probabilistic seismic hazard maps for New Zealand (Stirling et al., 2002). The 2015 RMS model, based on Stirling et al., (2012) will update several key source parameters including: implementation of the new set of crustal faults which now includes over 500 individual fault sources, a new time-dependent model for Wellington, Ohariu, Wairarapa, and Alpine faults, multi-segment ruptures, updating the Hikurangi subduction zone geometry and recurrence rate (Wallace, 2009; Williams et al., 2013) and implementing new background rates with a robust methodology for modelling background earthquake sources. We compare return period hazard changes between our previous and updated models. A range of factors drive changes to the hazard and risk profiles in the main population centres. Auckland lies in the lowest hazard region where we don't have a lot of information about the location of faults. Distributed seismicity is modelled by averaged Mw-frequency relationships on area sources thus small changes to the background rates can have a large impact on the risk profile for the area. On the other hand, the risk in Wellington is particularly sensitive to how the Hikurangi subduction zone and the Wellington fault are modelled. Minor changes on these sources have substantial impacts for the risk profile of the city and the country as a whole.

1 SOURCE MODEL CHANGES

1.1 Crustal Sources

Recent years have seen a lot of debate on the characteristic earthquake hypothesis on strictly segmented faults. Recent events had rupture propagate beyond segment boundaries (e.g., Denali), which means that a given segment may have partial ruptures in combination with nearby segments. This complicates the inference of a fault-specific magnitude-frequency relationship. Likewise, renewal models, which assume that it takes time to reload a fault after a large rupture and therefore promote low probabilities of occurrence right after a large event, were put into question. Experiments have been carried out to characterize seismic activity at the regional scale using a purely unsegmented approach (e.g., UCERF3). The Gutenberg-Richter (GR) frequency-magnitude relationships reflects the situation in which events of all magnitudes between a minimum and a maximum magnitude are possible in the system, with a fixed proportion of small to large events (the b-value). The constraints for a GR relationship for individual faults were abandoned and only regional GR were enforced, allowing a characteristic event-type relationship for individual faults. However the criteria used to unsegment the event set are still to be refined to comply with geologic observations. Also the correlation of event occurrences between nearby faults is ignored.

In the update to our New Zealand (NZ) risk model, we opted for 1) maintaining a mostly segmented model to take full advantage of the detailed characterization of past events, 2) coupled with a relaxed assumption regarding recurrence models, in which we find the best combination of known functional forms that fit the data. This allows us to have a significant component of short-term recurrence (Poisson-like or even more clustered) as well as a main renewal-type optimum for time to failure. 3) Those

models were fitted to individual faults, but in densely faulted regions with mature faults the regional pattern of occurrence of events was preserved. This is particularly important since our model will be simulation-based. 4) Finally, we used the openSHA tool designed to create the event set in UCERF3, together with local expert knowledge on the various fault systems, to introduce a meaningful but in no way exhaustive set of multiple segment ruptures. Those rare large events are critical for risk assessment. The boolean response to the distance between segments was relaxed since long jumping distances were observed in NZ, the cumulative azimuth change was reduced and some structural barriers such as the Cook Strait Canyon were deemed more important than the jumping distance.

1.1.1 *Time-independent Faults*

The time-independent crustal fault component in RMS' new NZEQ risk model is based on the GNS 2010 NZEQ hazard map products. Stirling et al. (2012) specify that the fault source model uses the dimensions and slip rates of mapped fault sources to develop a single characteristic earthquake (magnitude and frequency) for each fault source, while the spatial distribution of historical seismicity is used to develop Gutenberg–Richter magnitude–frequency estimates for the distributed seismicity model. More details of RMS' background source development can be found in section 2.3.

The 2010 national seismic hazard map benefited from the addition of about 200 faults and the revision of the slip rate and sometimes the geometry of many of the existing sources. In particular, a large number of faults were added in the Taupo rift region and in the Havre Trough region.

To determine the characteristic magnitude of each mapped fault, assumed to rupture independently from their neighbors, a new set of scaling relationships was applied. The equation of Hanks and Bakun (2002) was chosen for the plate-boundary strike-slip faults (e.g., the Alpine fault). The equation by Villamor et al. (2007) was applied to shallow normal faults and normal faults in rift or volcanic environments. Finally, the equation by Stirling et al. (2008) was used for all remaining faults. Note that while the first two relationships depend directly on rupture area, the third one explicitly separates the effect of down dip width from that of length.

There are two main differences between RMS' and GNS' models for those sources. First, an uncertainty around the characteristic magnitude was allowed, such that the moment defined by GNS is conserved for each source. Second, the Wairarapa 1855 event was revisited based on the The 1855 Wairarapa Earthquake Symposium proceedings (Townend et al, 2005) and on a historical reconstruction. The 1855 event is inferred to have involved the Wairarapa fault, a shallow Wharekauhau thrust and part of the subduction interface.
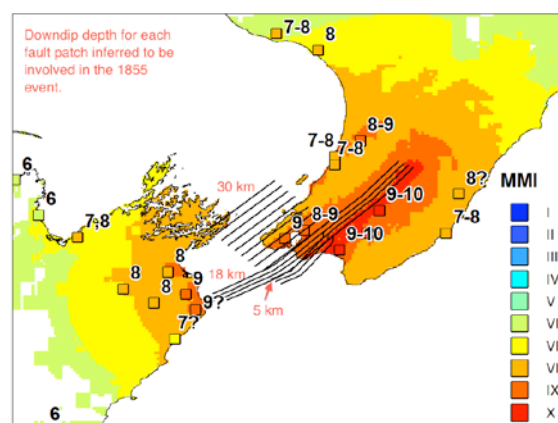

Figure 1. Contour lines of the new geometrical representation of the 1855 Wairarapa earthquake, validated against macroseismic intensities computed using McVerry's attenuation law (color scale) and from macroseismic surveys (colored squares). The rupture involves the Wairarapa fault, a shallow Wharekauhau thrust and part of the subduction interface.

1.1.2 *Time Dependent Faults*

Rhoades et al. (1994) pioneered the use of Bayesian inference and the use of geologically-based priors on mean recurrence time into the characterization of renewal models for hazard computation. Following that methodology, Rhoades et al. (2011) and Van Dissen et al. (2013) incorporated slip rate and slip per event distributions fitted to field measurements and used a Bayesian method to incorporate and propagate uncertainties on earthquake dates from trenches and prior information, and combine the PDFs of the chosen renewal according to the posterior of the model parameters. Instead of using several logic-tree branches each with the hazard rate steming from each renewal model, Van Dissen et al., (2013) proposed to use a mixture of the hazard rate from several renewal models to account for epistemic uncertainties. Stirling et al (2012) used the 50 and 100 year average hazard rates in the time-dependent national seismic hazard map (NSHM).

Fitzenz and Nyst (2015, later referred to as FN15) describe the method used in RMS' risk model.

Using a Bayesian method means working with a predefined dataset, all elements of the problem are random variables, and one cannot know whether the model is true and whether there is a true value for its parameters. One can only say that assuming the candidate models are true, the data provide the relative plausibility of each model as well as the posterior probability of the parameters for each model. There is an inherent, unknown, epistemic uncertainty to the problem, in that there might be better suited models that were not incorporated. This last point is also found in logic-tree methods because, to form a valid logic tree, all branches need to be collectively exhaustive, which one cannot know as far as renewal models are concerned.

 The method in FN15 is similar to that of Rhoades et al. (1994) but differs from it in three main points. First, it does not require the sampling of distributions: an analytical formulation is used whenever possible, and numerical integration (or marginalization) is preferred to sampling. Second, the geomorphology data is used to build a prior on mean recurrence time and a uniform prior on CV, and the likelihood of both the CV and the mean recurrence time is computed using the trench data. This is in contrast to Rhoades et al. (1994), who use a uniform prior on CV and calculate the likelihood of CV for each vector of interevent times and associated sample of mean recurrence time (from geomorphology). One of the consequences of these choices is that the state of knowledge on the mean recurrence time is updated using the trench data in FN15 method, not in theirs, because they deem that the dated cumulative offsets and slip per event from geomorphology bring more reliable information on the long-term mean recurrence time than the trench data. Third, after FN15 get the posterior probability for the parameter space for each model, they go on to compute the average PDF of each model PDF weighted by their Bayes factor. It is only once they have the Bayesian optimal model combination (in terms of PDF) that they compute the hazard rate function. On the contrary, Van Dissen et al. (2013) compute the hazard rate function for each model, choose arbitrary model weights, and then compute their combined hazard rate function. Table 1 presents the equivalent return periods and the integral of the conditional probabilities for the three faults studied in Van Dissen et al. (2013) and FN15. The equivalent return period at a point in time is the inverse of the hazard rate. Similarly one can define an equivalent return period over some period (e.g., 5 years, 100 years). In that case it is the inverse of the integral of the conditional probability over that period. Those are defined by analogy to the long-term recurrence time being the inverse of the long-term rate of occurrence.

Table 1. Summary of equivalent return periods (computed using the integral of the conditional probabilities given in (), using the computed model weights) after Fitzenz and Nyst 2015.

Model	Wellington-Hutt	Wairarapa 1855	Ohariu	Alpine
Mixture of models, 1 yr average 2010	2366.5 yr ($4.225 \ 10^{-4}$)	15,736 yr ($6.35 \ 10^{-5}$)	2438 yr ($4.1 \ 10^{-4}$)	-
Mixture of models, 100 yr average, starting 2010	2054 yr (0.0475)	10,904 yr (0.0090)	2,334 yr (0.0419)	-
Model Weights	39.7% BPT 22.9% Weibull 37.4% lognormal	31.1% BPT 36.5% Weibull 32.4% lognormal	33.2% BPT 33.1% Weibull 33.7% lognormal	7.5% BPT 79.34% Weibull 13.15% lognormal
2010 NSHM 1 yr average 2010 50% BPT 20% Weibull 30% lognormal	($10.0 \ 10^{-4}$)	($1.9 \ 10^{-4}$)	($4.8 \ 10^{-4}$)	($2.9 \ 10^{-3}$)
NZEQ07 (BPT only, aperiodicity 0.5), yr 2010	411.5 yr	99,814 yr	15,278 yr	169 yr
Next 5 year average hazard rate	($4.35 \ 10^{-4}$)	($6.83 \ 10^{-5}$)	($4.13 \ 10^{-4}$)	($6.18 \ 10^{-3}$)
5-year average after event occurrence (beginning of cycle)	($6.44 \ 10^{-5}$)	($7.32 \ 10^{-6}$)	($2.19 \ 10^{-5}$)	($7.60 \ 10^{-6}$)

Paleoseismological records exist for several other crustal faults in New Zealand in or around the Cook Strait (such as Wairau and Awatere, Pondard et al. 2010). Recent or ongoing lidar survey interpretations are also yielding new information on cumulative fault offsets and slip per event to supplement field and aerial photography studies (Hope fault, Langridge and Berryman, 2005). When put together, the trench dates seem to be records of participation in a large event and the slip per event seem to indicate larger slip than would be expected for individual segments. More work needs to be done to infer the rupture length and tips. Earthquake geology and geomorphology, as well as the study of lake sediments (Howarth et al., 2012) will play a big part in defining how those records are used in the future.

Finally, the southern Alpine fault has been the focus of a lot of research (Berryman et al., 2012; Biasi et al. 2015). Statistical analysis of the 22 consecutive events encountered in trenches (Berryman et al., 2012) yielded an aperiodicity on the order of 0.33, indicating a more periodic behavior than commonly inferred for crustal faults around the world. However, recent probabilistic studies (Biasi et al., 2015) show that when a renewal model is assumed (be it lognormal or Brownian Passage Time), the likelihood of the model parameters knowing the data is maximum for aperiodicities around 0.45. We are collecting geomorphological data similar as those used to build priors for the three faults near Wellington so that we can apply the same overall methodology while using the most up-to-date and sophisticated likelihoods. Integrating over the posterior probability mixes models with even higher aperiodicities, so even though the mean recurrence time is on the order of the time since the last major event on that fault, a smaller hazard rate is expected, than in a case with a small aperiodicity. We obtain a hazard rate averaged over the next 5 years equivalent to a return period of 162 years, when the long-term rate used in the 2010 NSHM is 340 years (Table 1).

1.1.3 *Multi-Segment Ruptures*

Longer (than 475 year) return period losses need to be defined to compute risk metrics for capital requirement calculation. The 2010 NSHM includes long return period events only far from exposure (mostly in the South Island, e.g., Hump Ridge, 63240 yr or Old Man, 362150 yr).

We adapted the tool developed by UCERF3 within OpenSHA to generate a rupture set using an unsegmented fault model. UCERF3 compiled field observations and earthquake simulator results to come up with a set of rules to link up fault sections into potential ruptures.

First, all faults are discretized in short fault elements (called subsections) of about half their average down-dip width.

The following tests are applied to these subsections (Milner et al., 2013) :

1. The shortest distance between 2 fault sections is 5 km or less
2. Strikes cannot vary by more than some amount between neighboring subsections (e.g., 60º)
3. Strikes cannot change by more than some total amount along the rupture length (e.g., 560º)
4. Rakes cannot change by more than some amount between subsections (e.g., 180º=maxCum)
5. Ruptures cannot include a given subsection more than once (e.g., preventing ruptures from looping back on themselves)
6. Rupture on previous subsection results in increase in Coulomb Failure Stress (CFS, no threshold value, just >0)

We opted to use criteria 1 to 5, although Pondard et al. (2010) computed CFS for most faults around and in the Cook Strait area and this work could be used as a basis to build the table needed in OpenSHA. To get the magnitude of the events, the proper length-magnitude or area-magnitude scaling has to be selected (see compilation in Stirling et al. 2012).

We investigated the impact of

- linkage between the Alpine fault plate boundary, faults in the Marlborough system, and the North Island Dextral Fault Belt,
- linkage between N. Marlborough faults and the contractional Kapiti and Manawatu fault zones
- linkage of all Kerepehi normal fault segments,
- linkage between the North Island Dextral fault belt and the onshore and offshore rift normal faults in the Bay of the Plenty.

We paid particular attention to those faults that were shown to rupture in sequences (event dates in succession) or for which the probability density function for the date of their events overlap between an event on one fault and an event on the neighboring fault. In those cases, events might have happened in sequence, or even coseismically. We assigned larger frequencies to multiple-segment ruptures representing coseismic cascades in those locations. We also introduced a small number of very long ruptures, geometrically possible but for which there is no supporting dataset. We assigned them a 100,000 year recurrence interval.
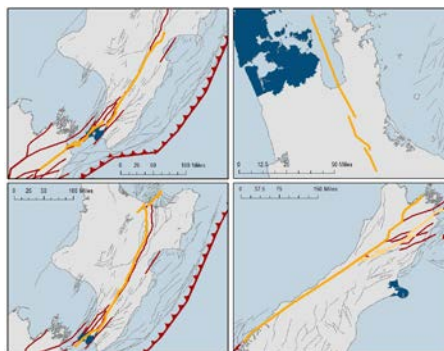

Figure 2. A subset of possible combinations of segments. Geometric considerations suggest large earthquakes can cross the Cook Strait.

1.2 Subduction Zone

Stirling et al. (2012) published new maximum magnitude assumptions on the Hikurangi interface in reaction to the occurrence in 2011 of the (unmodeled) Tohoku event. The maximum magnitude is now 9 and corresponds to a "full subduction zone" event. New science allows for detailed mapping of geometry subduction zone (Contours Hikurangi Subduction Zone from Williams et al., 2013). Figure 3 shows how RMS uses both the overall characterization by Stirling et al., 2012 and the new contours by Williams et al, 2013) to model this M9 event, from the trench down to the 33 km contour below trench level.

Stirling et al. (2012) also propose that the subduction ruptures in parts, roughly 300 to 500 km in length, in events between 8.1 and 8.5. The coupling of the subduction interface changes from North to South (Wallace et al., 2009), with a narrower zone of stress accumulation in the North, but no barrier to slip has been evidenced so far. On the other hand, the 2007 NZEQ model included subduction events with a characteristic magnitude between 7.5 and 8.4 with a +/- 0.2 magnitude uncertainty. For consistency, RMS' new implementation therefore includes "floating" events (Mw 7.6 - 8.6) that rupture parts of the subduction zone, preserving but not limited to, the segment boundaries defined by Stirling et al. (2012) in terms of their lateral extent, and with a down-dip limit between the 27 and 30 km contours depending on the magnitude.

Note that the rates of events occurring on the subduction interface increase in Stirling et al. (2012) compared to the 2002 New Zealand National Seismic Hazard Map. RMS' interpretation preserves the moment rates prescribed by Stirling et al., 2012. The net result is that one can expect a larger influence of the subduction on the Wellington region losses compared to previous models.
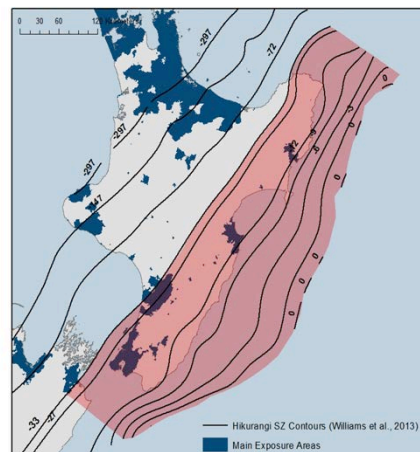

Figure 3. Extent of the modeled M9 event on the Hikurangi subduction interface in RMS' new source model.

1.3 Background

In addition to faults and subduction zone sources we also allow the possibility of earthquakes to occur anywhere within the country on potentially inactive or unmapped faults. These so-called background sources are modelled as pseudo-faults ranging from M_W 4.8 to 7.4 with lengths consistent with their seismotectonic region.

1.3.1 *Rates*

Rates of occurrence for these background faults are based on the rates developed by GNS for the 2010 National Seismic Hazard Map (NSHM) (Stirling, et al., 2012). Occurrence rates were developed using an earthquake catalogue ranging from 1964 to July 2009. Older data was excluded due to the large

uncertainties in the magnitude, location and depth.

At the time of this paper GNS released updated rates for the Canterbury region based on Gerstenberger et al., 2014. (http://www.gns.cri.nz/Home/Our-Science/Natural-Hazards/Earthquakes/Earthquake-hazard-modelling/Canterbury-SHM). These rates represent yearly forecasts up to 50-years. While current occurrence rates are based on the GNS 2010 NSHM, we are investigating these rates and are considering using them in our time dependent model.

1.3.2 *Faults*

This section describes the new background source component in RMS' earthquake risk models. Rather than designing the background source location and orientation in a uniform way, the new source locations are randomly distributed across specific areas. The orientations of the faults follow a prescribed strike angle with a random deviation from the prime orientation, determined by sampling from the uncertainty in the orientation. In this way we enhance the stochastic nature of the background event set from the previous background source development method.

Rather than prescribe uniform background fault locations we determine fault centroid locations by sampling from the area within the background source zone. However, if locations are sampled using a purely random method, spatial gaps or clustering may occur within the sample zone. Although randomness in source locations is desired, the sources should also be evenly distributed in such a way to uniformly define seismic hazard within the entire zone. For this reason, instead using purely random sampling we use a Latin Hypercube sampling (LHS) method that considers the location of all sampled fault centroids by minimizing the 2D correlation between points while considering the total number of points to be sampled. This preserves a level of randomness, while at the same time limiting the number of clusters and gaps in event locations.

Orientation and size of background sources should reflect the regional seismotectonics. Geologic, geophysical, and seismologic data are all used to constrain these parameters. The orientations of pre-existing faults are used to constrain the orientation of crustal background sources. If these faults don't exhibit any seismic activity, they can be considered inactive in a neotectonic (i.e., recent or current) sense. However, if regional tectonic stress builds up, reaches a certain threshold and the fault has a favourable orientation for stress release, it's not unlikely that an earthquake could occur on those faults or on nearby faults with similar structure. Geophysical data (e.g. stress orientations) supplement geologic data and can further constrain potential orientations of background events. The World Stress Map (Heidbach et al., 2008) is a compilation of stress orientations from around the world. In addition to the fault and stress data we also use orientations calculated from seismograms of recent earthquakes. These focal mechanisms (nodal planes) are derived from the moment tensor solutions of moderate and large earthquakes (Ekström et al., 2012) and provide insight into the orientation of the rupture surface. If there are enough nodal planes in the zones distributions of orientations can be estimated. The combination of all of this data is then used as a guide to prescribe the orientation and the associated uncertainty per background source area. The final orientations and uncertainties for New Zealand are shown in the Figure 4.
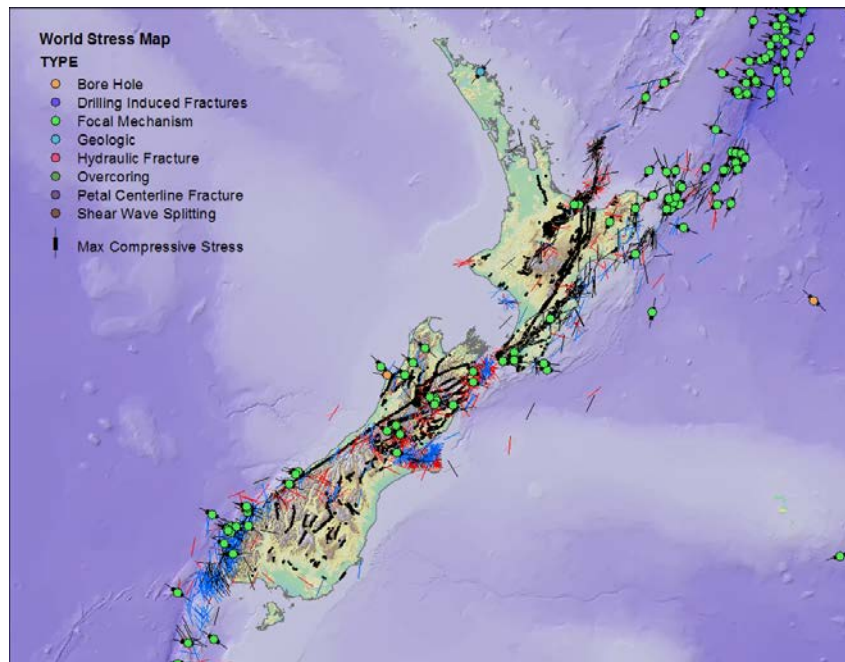
Figure 4. World Stress Map (Heidbach et al., 2008) orientations, focal mechanism nodal planes (Ekström et al., 2012) and Quaternary faults shown for New Zealand are all used to help establish the preferred orientations for the background zones.
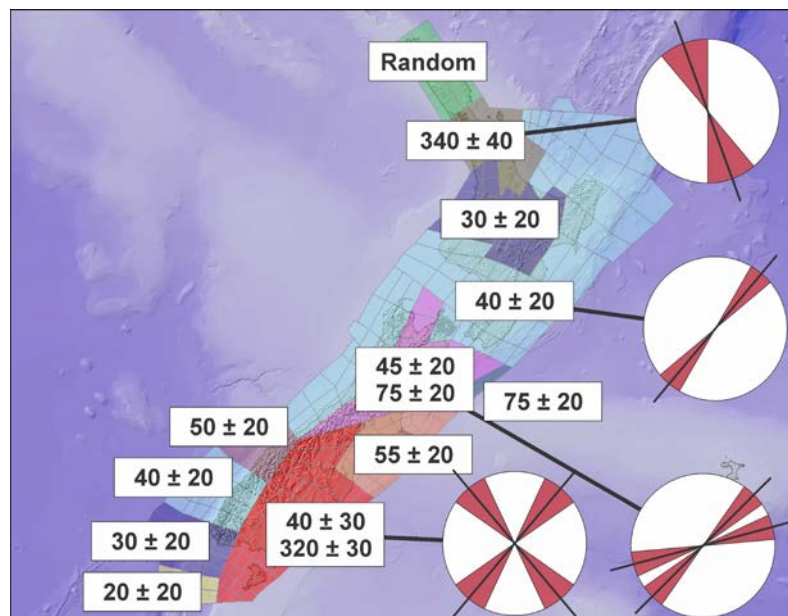

Figure 5. Final preferred orientations for the background zones in New Zealand. Each number represents an azimuth and the associated uncertainty. The reported uncertainties show here are 2-sigma uncertainties. In some zones conjugate fault orientations are represented with two values.

The orientation distributions for each zone are discrete and typically separated into bins of 1, 2, or 5 degrees. We then sample an orientation direction (azimuth) for each of the fault locations in a zone without replacement. Because the sample size is not significantly large, sampling without replacement ensures that the final distribution of orientations matches the a priori distribution. As the sample size grows we capture increased variability by reducing the orientation bin size.

Once location and orientation have been sampled we compute the length of the background event based on magnitude. Magnitude-length or magnitude-area relationships must be used in order to compute a fault source length. Stirling et al., (2013) highlights a number of different magnitude-length

and magnitude-area relationships by various authors from around the world. Many relationships exist for relating fault rupture length to the event magnitude. The relationship used to compute the fault length must be based on the global location, tectonic regime, and faulting style.
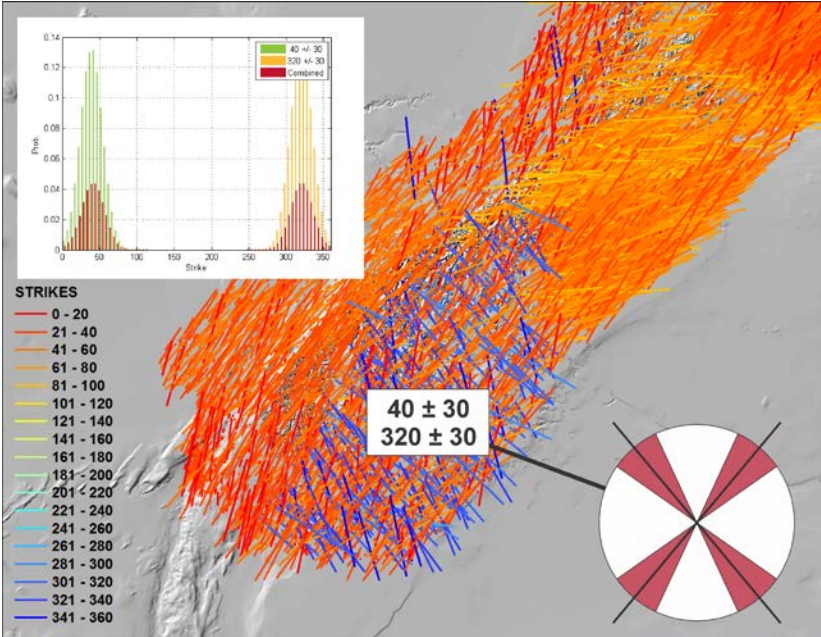

Figure 6. Two preferred orientation in southern New Zealand. The inset figure on the top left shows the distribution of the strikes sampled for the region (40±30 and 320±30). The inset figure on the bottom right shows the orientations and 1-sigma uncertainties. The two orientations can be distinguished by color in the region. Blue faults are orientated approximately northwest (azimuth 320) and the orange faults are orientated approximately northeast.
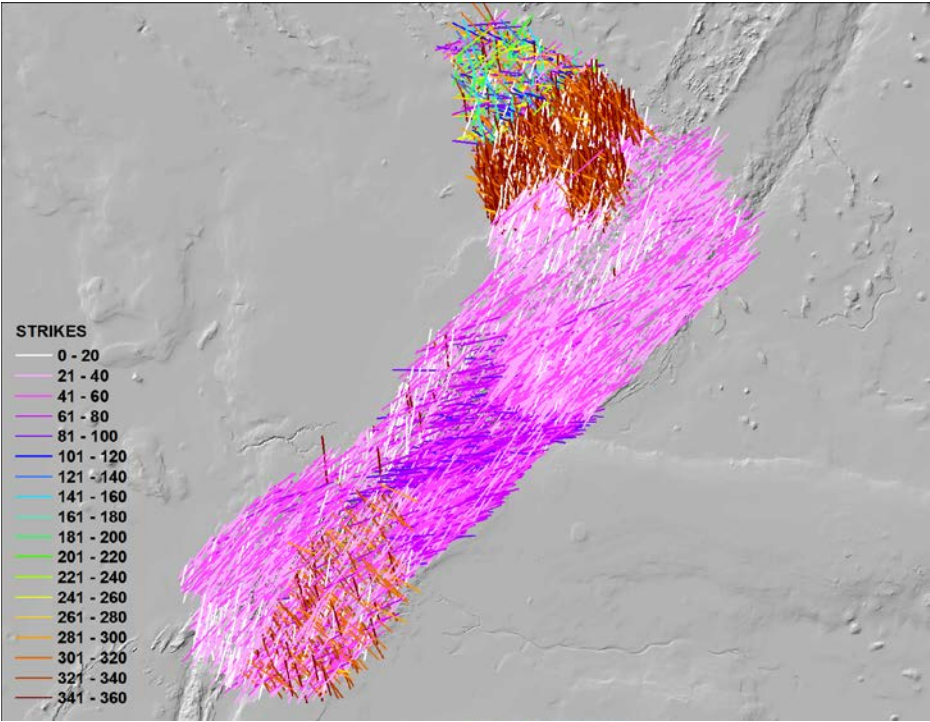

Figure 7. The final 10 km layer in the New Zealand background model. Color changes on the faults show the changes in orientation. Note the rainbow colors in the northwest which show purely random orientations.

2 HAZARD AND RISK CHANGES

Ground motion estimates (Figure 8) from PSHA help define the building code required to prevent buildings from killing people, risk models help insurers and re-insurers remain solvent and guarantee that those insured will be able to move on, adapt and rebuild when and where the earthquakes strike. We use two primary risk metrics, average annual loss (AAL) and Exceedance Probabilities (EP), analogous to ground motion hazard curves. The AAL is the expected loss per year averaged over the return period and is used in the establishment of insurance premiums. It is more sensitive to the shortest return period events, so that premiums are computed on the basis of the losses due to the most frequent events (typically not the largest events). This is the primary metric we analyse when testing different background rates.
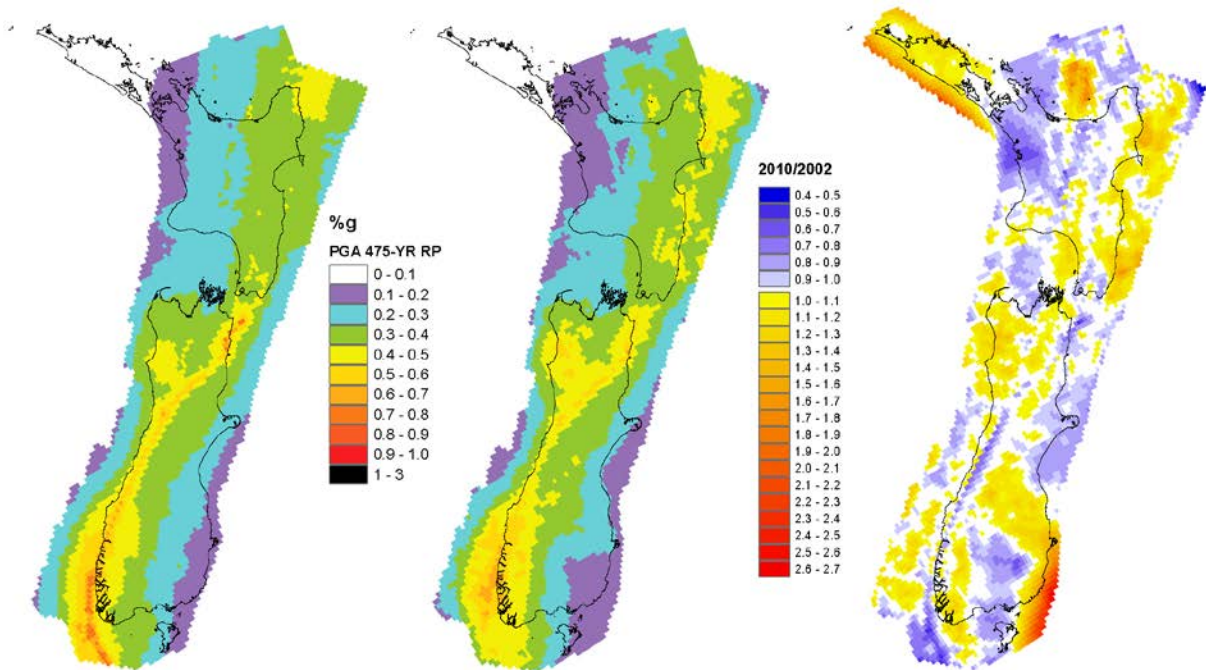

Figure 8. Peak Ground Acceleration (PGA) at a return period of 475 years for the GNS 2002 model (left) and the GNS 2010 model (center). The ratio map of GNS 2010 to GNS 2002 PGA values is shown on the right.

We evaluated the changes in earthquake risk considering the current and former source models. Changes in risk were captured as the percent change, as compared to the rates from GNS (Stirling et al, 2012), in expected (ground up) loss to insured property, as defined in the RMS® New Zealand Industry Exposure Database (IED). For each zip code, RMS has developed estimates of total insured values using a variety of sources, including census demographics and economics data, building square footage data, and representative policy terms and conditions. In essence, the personal (residential and cooperative), commercial, and industrial lines of businesses were analysed against each new view of hazard. We grouped exposure from all zip codes for each of the three cities in our analysis. We computed the ground up loss for each city using the GNS 2010 rates (Stirling et al., 2012). We then compare the change in loss from the rates derived from the previous model. Looking at the contribution to average annual loss by source type for the all exposure in the country, we note the shift in perspective from the Wellington fault dominated old model (GNS 2002) to the current model where the subduction zone dominates the risk. We also calculated the return period loss costs (ratio of losses by exposure value). Those are the loss costs that are exceeded at a probability equal to one over the return period. Since 1) the recurrence on the Wellington fault was inferred to be larger than previously thought, 2) rare multiple-segment events were added to the source model, and 3) the subduction zone events have recurrences between about 500 years for the Wellington segment to thousands of years for the M9 event, the new source model brings the high return period (>500 years) loss costs to a higher level than the previous model.

3 CONCLUSION

Whereas Probabilistic Seismic Hazard Assessment helps define the building code required to prevent buildings from killing people, risk models help insurers and re-insurers remain solvent and guarantee that those insured will be able to move on, adapt and rebuild when and where the earthquakes strike. For a given portfolio (sites with location, value, and building characteristics), losses are defined for each event according to a financial model. Those losses, together with the frequency of the events, are used to compute a number of loss metrics. Those metrics are used to inform re/insurers about the accumulation of insured locations in risk areas, the average annual loss which serves as a basis for computing premiums, and the exceedance probability curve.

The RMS earthquake source model for RMS' New Zealand earthquake risk model is based on that developed for the National Seismic Hazard Map (Stirling et al. 2012). It is then extended to incorporate data updates (such as the recently published contours of the Hikurangi subduction zone) and to better suit the needs of a risk model in terms of event characterization and uncertainty assessment and propagation. It is very important to incorporate as many different realizations of an event as necessary to cover the uncertainties in location, orientation, magnitude, frequency. This led to innovative work for time-dependence, for background source development, for the Hikurangi source development. It also led to the addition of magnitude uncertainty on all crustal sources,

Preliminary loss results show that, in view of recent geological evidence, the Wellington-Lower Hutt Valley fault is no longer the main driver of losses in the Wellington region and in New Zealand. Instead, both the Wellington fault and the subduction zone need to be taken into account. Final loss results will incorporate updates to many other components of the risk model. Those include updates to the liquefaction potential, vulnerability curves, and the New Zealand Industry Exposure Database.

4 REFERENCES

Berryman, K., U. Cochran, K. Clark, G. Biasi, R. Langridge, and P. Villamor (2012). Major earthquakes occur regularly on an isolated plate boun- dary fault, Science 336, no. 6089, 1690–1693.

Biasi, G., P., R. M. Langridge, K. R. Berryman, K. J. Clark, and U. A. Cochran, 2015, Maximum-Likelihood Recurrence Parameters and Conditional Probability of a Ground-Rupturing Earthquake on the Southern Alpine Fault, South Island, New Zealand, Bull. Seis. Soc. Am.,, Vol. 105, No. 1, pp. 94–106, February 2015, doi: 10.1785/0120130259

Ekström, G., M. Nettles, and A. M. Dziewonski, The global CMT project 2004-2010: Centroid-moment tensors for 13,017 earthquakes, Phys. Earth Planet. Inter., 200-201, 1-9, 2012. doi:10.1016/j.pepi.2012.04.002

Field, E. H., G. P. Biasi, P. Bird, et al., 2013. Uniform California Earthquake Rupture Forecast, Version 3 (UCERF3)—The Time-Independent Model, U.S.G.S. Open File Report 2013-1165.

Fitzenz, D.D., and M. Nyst, 2015. Building time-dependent earthquake recurrence models for probabilistic risk computations, Bull. Seis. Soc. Am., Vol. 105, No. 1, pp. 120-133, February 2015, doi: 10.1785/0120140055.

Matthew Gerstenberger, Graeme McVerry, David Rhoades, and Mark Stirling (2014) Seismic Hazard Modeling for the Recovery of Christchurch. Earthquake Spectra: February 2014, Vol. 30, No. 1, pp. 17-29.

Hanks, T. C., and W. H. Bakun (2002). A bilinear source-scaling model for M-log A observations of continental earthquakes, Bull. Seismol. Soc. Am. 92, 1841–1846.

Heidbach, O., Tingay, M., Barth, A., Reinecker, J., Kurfeß, D., and Müller, B., The World Stress Map database release 2008 doi:10.1594/GFZ.WSM.Rel2008, 2008.

Howarth, J.D., Fitzsimons, S.J., Norris, R.J., and Jacobsen, G.E. 2012. Lake sediments record cycles of sediment driven by large earthquakes on the Alpine Fault, New Zealand. Geology, v. 40, p. 1091-1094.

Langridge and Berryman, 2005. Morphology and slip rate of the Hurunui section of the Hope Fault, South Island, New Zealand, New Zealand journal of geology and geophysics 48 (1), 43-57

Milner, K., M.T. Page et al., 2013. Appendix T—Defining the Inversion Rupture Set Using Plausibility Filters, UCERF3 working group final report, 2013.

Pondard, N. and P. M. Barnes (2010) Structure and paleoearthquake records of active submarine faults, Cook Strait, New Zealand: Implications for fault interactions, stress loading, and seismic hazard, J. Geophys. Res., DOI: 10.1029/2010JB007781

Rhoades, D. A., R. J. Van Dissen, and D. J. Dowrick (1994). On the handling of uncertainties in estimating the hazard of rupture on a fault segment, J. Geophys. Res. 99, no. B7, 13,701–13,712.

Rhoades, D., R. Van Dissen, R. Langridge, T. Little, D. Ninis, E. Smith, and R. Robinson (2011). Re-evaluation of conditional probability of rupture of the Wellington-Hutt valley segment of the Wellington fault, Bull. New Zeal. Soc. Earthq. Eng. 44, no. 2, 77–86.

Stirling, M. W., G. H. McVerry, and K. R. Berryman (2002). A new seismic hazard model of New Zealand, Bull. Seismol. Soc. Am. 92, 1878–1903.

Stirling,M., M. Gerstenberger, N. Litchfield, G. McVerry, W. Smith, J. Pettinga, and P. Barnes (2008). Seismic hazard of the Canterbury region, New Zealand: New earthquake source model and methodol- ogy, Bull. New Zeal. Natl. Soc. Earthquake Eng. 41, 51–65.

Stirling, M., G. McVerry, G. and M. Gerstenberger et al. (2012), National seismic hazard model for New Zea-land: 2010 update, Bull. Seis. Soc. Am., 102(4), doi: 10.1785/0120110,170.

Stirling, M., Goded, T., Berryman, K., Litchfield, N., Selection of earthquake scaling relationships for seismic-hazard analysis. Bulletin of the Seismological Society of America (December 2013), 103(6):2993-3011

Townend, J.; Langridge, R.M.; Jones, A. (comps) *The 1855 Wairarapa Earthquake Symposium : 150 years of thinking about magnitude 8+ earthquakes and seismic hazard in New Zealand : 8-10 September 2005 : proceedings volume.* [Wellington, NZ]: Greater Wellington Regional Council.

Van Dissen, R., D. A. R. Rhoades, T. Little, R. C. N. Litchfield, and P. Villamora (2013), Conditional probabil-ity of rupture of the Wairarapa and Ohariu faults, New Zealand, New Zealand Journal of Geology and Geophys-ics, 56(2), DOI:10.1080/00288,306.2012.756,042.

Villamor, P., R. Van Dissen, B. V. Alloway, A. S. Palmer, and N. Litchfield (2007). The Rangipo fault, Taupo Rift, New Zealand: An example of temporal slip-rate and single-event displacement variability in a volcanic en-vironment, Geol. Soc. Am. Bull. 119, 529–547.

Wallace, L. M., et al. (2009), Characterizing the seismogenic zone of a major plate boundary subduction thrust: Hikurangi Margin, New Zealand, Geochem. Geophys. Geosyst., 10, Q10006, doi:10.1029/2009GC002610.

Williams, C.A., Donna Eberhart Phillips, Stephen Bannister, Daniel H. N. Barker, Stuart Henrys, Martin Reyners, and Rupert Sutherland 2013, Revised Interface Geometry for the Hikurangi Subduction Zone, New Zealand, Seismological Research Letters doi: 10.1785/0220130035 v. 84 no. 6 p. 1066-1073